European Journal of Orthodontics 35 (2013) 38–44
doi:10.1093/ejo/cjr050
Advance Access publication 29 March 2011

Precision of identifying cephalometric landmarks with cone beam computed tomography *in vivo*

Bassam Hassan*, Peter Nijkamp**, Hans Verheij*, Jamshed Tairie*, Christian Vink**, Paul van der Stelt* and Herman van Beek**

*Section of Oral Radiology and **Department of General and Specialized Dentistry, Section of Orthodontics, Academic Centre for Dentistry Amsterdam (ACTA), Amsterdam, The Netherlands

Correspondence to: Bassam Hassan, Section of Oral Radiology, General and Specialized Dentistry, Academic Centre for Dentistry Amsterdam (ACTA), Amsterdam, The Netherlands. E-mail: b.hassan@acta.nl

SUMMARY The study aims were to assess the precision and time required to conduct cephalometric analysis with cone-beam computed tomography (CBCT) *in vivo* on both three-dimensional (3D) surface models and multi-planar reformations (MPR) images. Datasets from 10 patients scanned with CBCT were used to create two types of images: 1. axial, coronal, and sagittal MPR images and 2. 3D surface models. Eleven observers identified 22 cephalometric landmarks on 3D surface models first and then using 3D in combination with MPR images twice independently. Tracing time was recorded in both methods. Precision was defined as the absolute difference between an observer's repeated measurements and the mean of all measurements per landmark. Inter- and intra-observer agreements were defined as the absolute difference of the observers' measurements from each other and from their repeated measurements averaged over all landmarks, respectively. The precision of measurements ranged between 0.29 ± 0.17 and 2.82 ± 7.53. Adding MPR alongside, 3D surfaces improved the precision of tracing for 15 of 22 of the landmark but it took on average twice as much time. Mean time required to trace one patient was 6:03 ± 2:48 and 10:41 ± 4:01 minutes for 3D and 3D + MPR, respectively ($P = 0.0001$).

Introduction

In three-dimensional (3D) cephalometric analysis, anatomical landmarks are identified on 3D surface-rendered models obtained from computed tomography (CT) scans. In this tracing method, cephalometric planes are defined using either three or four landmarks instead of the two landmarks conventionally employed in two-dimensional (2D) cephalometry (Olszewski *et al.*, 2006; Swennen *et al.*, 2006 a,b). The stated advantages of this method over 2D cephalometric analysis include the elimination of the superimposition of bilateral structures and unequal enlargement artefacts and the ability to evaluate the right and the left sides of the skull independently (Kragskov *et al.*, 1997; Halazonetis, 2005). However, the adoption of 3D cephalometric analysis for routine orthodontic cases remains hitherto limited due to cost and accessibility constraints and increased radiation dose delivered to the patient that using CT in orthodontics is largely confined to severe asymmetry cases (Maeda *et al.*, 2006). Understandably, Multi-Slice CT (MSCT) systems available in radiology departments in general hospitals and private imaging centres are largely inaccessible to most orthodontists on routine basis. In addition, the relatively increased scan cost and radiation dose delivered to the juvenile orthodontic patients' population cannot be ethically and legally justified. As a result, using MSCT for cephalometric analysis of routine orthodontic cases is largely deprecated.

The introduction of cone-beam computed tomography (CBCT) in the past decade in dental radiology and its wide adoption for many clinical applications in dentistry revived the interest of employing 3D cephalometric analysis for routine orthodontic cases. CBCT offered decisive advantages over MSCT in terms of increased accessibility and decreased machine and scan costs (Kau *et al.*, 2005; Swennen and Schutyser, 2006). However, it is inappropriate to automatically state that CBCT delivers much lower radiation dose than MSCT for orthodontic applications although this was previously correct (Silva *et al.*, 2008). Recently, it was widely acknowledged that effective radiation dose with CBCT is variable with respect to the type of the scanner used, scan field of view (FoV) selected, number of projections acquired, detector characteristics, exposure mode, and scan settings plus other factors (Palomo *et al.*, 2008; Ludlow *et al.*, 2009; Roberts *et al.*, 2009). Moreover, latest generations MSCT offer low-dose 'dental scans' modes, which can offer image quality and radiation dose levels comparable to large FoV CBCT scanners (Suomalainen *et al.*, 2009). Yet, the advantages of smaller machines, reduced costs and increased accessibility of CBCT over MSCT, remain substantial.

CBCT acquires the patient head as a 3D volume, which can be used to create different 2D and 3D reconstructions (Arai *et al.*, 1999). The geometric accuracy of CBCT is

well established in the literature (Hilgers *et al.*, 2005; Marmulla *et al.*, 2005; Pinsky *et al.*, 2006; Lagravère *et al.*, 2008). Virtual 2D lateral cephalograms reconstructions from CBCT were found comparable in image quality to conventional 2D cephalograms (Moshiri *et al.*, 2007; Kumar *et al.*, 2007, 2008). For 3D cephalometric analysis, the precision of linear measurements made on CBCT 3D surface models based on dry skulls samples was recently reported to be within 0.5–2 mm when no reference markers were used (Periago *et al.*, 2008; Hassan *et al.*, 2009). When metallic reference markers were added, the precision was reported to be less than 0.5 mm (Berco *et al.*, 2009). However, using metallic markers largely invalidates the measurement procedure as it does not mimic the clinical situation *in vivo* and the position of the landmarks is arguably readily identifiable on the radiographs.

The quality of 3D surface-rendered models from CBCT depends on several factors including the type of scanner and detector used, scan FoV selection, segmentation threshold, and image artefacts (Loubele *et al.*, 2007, 2008 a,b). Visibility of cephalometric landmarks may vary among the different scanners and the different scanning and reconstruction parameters and depending on the threshold value selected for segmenting the 3D model. Dry skull samples neither account for the radiation attenuation caused by soft tissue nor do they account for the added partial object effect artefacts caused by the presence of structures (e.g. vertebrae) outside the scan FoV (Hassan *et al.*, 2010). This could overestimate the visibility of the cephalometric landmarks.

Thin slice, high contrast 2D axial, coronal, and sagittal multi-planar reformations (MPR) were thus added alongside the 3D surface models in a correlated view mode to improve the precision of identifying cephalometric landmarks. The measurement procedure involves identifying the landmark on the 3D model first and then adjusting the position using the MPR slices for added precision. This procedure has been recently used to quantify the precision of identifying cephalometric landmarks on CBCT *in vivo* (Chien *et al.*, 2009; De Oliviera *et al.*, 2009; Ludlow *et al.*, 2009). However, identifying landmarks on MPR images can be subjective and time-consuming process. Identifying the location of a landmark requires navigating through the stack of axial, coronal, and sagittal slices to identify the point in question and then finding the corresponding location on all three views. The visibility of the anatomical landmarks is additionally affected by the orientation of the head in the scanner and anatomical variations that in most cases bilateral landmarks are not visible on the same slice (Hassan *et al.*, 2009). The objective of this study is to assess the precision of and time required to identify cephalometric landmarks on CBCT *in vivo* on both 3D surface models and MPR images.

Materials and methods

Radiographic scans and sample preparation

The *in vivo* sample consisted of 10 patients (four males and six females and age range 18–23 years) pooled from a larger CBCT database of patients. The patient group was selected based on following criteria: (1) the permanent first molars, canines, and incisors were present bilaterally, (2) no orthodontic appliances or large metal restorations were present, and (3) no large facial asymmetry. An informed consent was obtained from the patients to use the data for research purposes. The patients were scanned with the image intensifier tube (IIT)/charge-coupled device (CCD) system NewTom 3G CBCT (QR SRL, Verona, Italy) with a 12 inch detector scan FoV. The scan position followed the manufacturer's recommendation with the patient lying flat on a table with the occlusal plane perpendicular to the floor. With the aid of laser markers, the midsagittal and occlusal planes were adjusted perpendicular to each other. Scans were made and datasets were exported according to the manufacturer's default settings in DICOM 3 file format at the isotropic voxel size of 0.3 mm. The datasets were 12 bits in depth, and the scaled gray values (212 = 4096) range was on average between −1024 and 3095.

Data analysis

The datasets were imported for analysis into Dolphin 3D software (version 11.0; Dolphin Imaging, Chatsworth, CA) and 3D surface models were created by selecting the solid (default) hard tissue rendering mode. In this mode, the software assigns a single global threshold value to segment the hard tissue from soft tissue to create and display an isosurface representation. A subjective threshold value was selected for each skull to segment bone from soft tissue and background.

Since small deviations in the position of the head from ideal are bound to exist, each patient's head position was corrected and re-aligned using Dolphin software tools using the midsagittal and Frankfort horizontal planes as references (Lundström *et al.*, 1995). The exact procedure to align 3D skull models from CT data has been previously described (Periago *et al.*, 2008; Hassan *et al.*, 2009; Ludlow *et al.*, 2009) with adaptation from the original method described by Swennen *et al.* (2006b). The procedure is as follows: 'using the coronal view, the volume was rotated medio-laterally until the transporionic line of the data was oriented horizontally (Figure 1a). Using the axial view, the volume was rotated until the midsagittal plane of the data was oriented vertically (Figure 1b). Using the sagittal view, the volume was rotated anterio-posteriorly until the Frankfort plane of the data was oriented horizontally (Figure 1c; Ludlow and Ivanovic, 2008)'. All adjustments to the sample were made by two investigators who were specially trained for this task and did not participate in the cephalometric tracing.

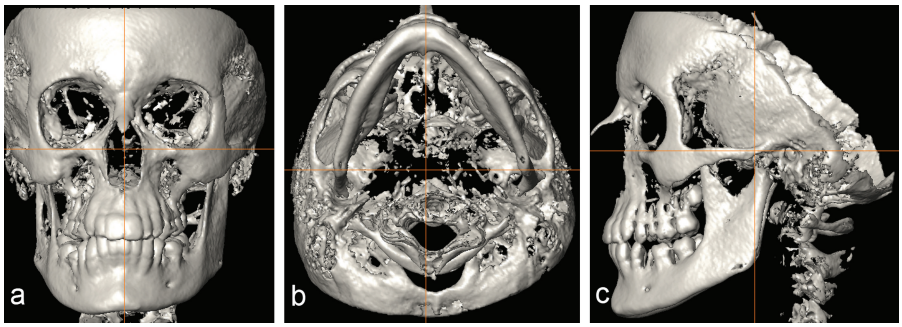

Figure 1 Alignment of the patient's head position in the scanner using the coronal (a), axial (b), and sagittal (c) views.

Study observers and cephalometric points

Eleven orthodontist residents were recruited as observers for this study. The observers were introduced and individually trained to use Dolphin 3D software to identify the cephalometric landmarks. The observers traced one dummy dataset five times on a 3D surface model and five times on a 3D model in combination with MPR images. The definitions of the 3D cephalometric landmarks were based on the points described by Swennen (2006). There were in total 22 cephalometric landmarks (Table 1).

Measurement procedure

Per patient, the observers were asked to identify each landmark in a specific order by selecting its name and clicking with the mouse on the landmark location. First measurement (3D) was made by utilizing only the 3D surface model. The observers were presented with a single window displaying the 3D surface model (Figure 2). Manipulating the 3D model by clipping, rotation, translation, and zooming was permitted in order to improve landmark's visibility. Adjusting the segmentation threshold value to improve the visibility of each individual landmark was also allowed. The digitized landmarks co-ordinates were then copied into Excel software (Version 2003; Microsoft, Redmond, Washington, USA). The time required to trace one individual patient was recorded using a stopwatch to designate the start and finish time of the tracing. Two investigators recorded the time and supervised the sessions but did not participate in or assist the observers with the cephalometric tracing. The second measurement (3D + MPR) was as follows: starting from the landmarks' co-ordinates on the 3D surface model from the first measurement, the observers were presented by a 4-panel window containing beside the 3D model also the axial, coronal, and sagittal slices in a correlated view (Figure 3). The observers were then asked to adjust and improve the position of the landmarks with the help of MPR images. All adjustments (e.g. clipping, zooming . . . etc) to the 3D model and to the MPR images were permitted as well. The new co-ordinates were digitized in excel and the additional time required to adjust the landmarks using MPR was also recorded following the same above mentioned procedure. To assess intra-observer reliability, each patient was traced twice in 3D and twice in 3D + MPR leading to a total of four tracings per patient. The patients were presented at random

Table 1 List of three-dimensional cephalometric points used in this study.

Structure	Definition
Or(R)	Orbitale right: most inferior point on the right infra-orbital rim
Or(L)	Orbitale left: most inferior point on the left infra-orbital rim
S	Sella turcica: centre of the hypophyseal fossa
N	Nasion: midpoint of the frontonasal suture
ANS	Anterior nasal spine: most anterior midpoint of the anterior nasal spine of the maxilla
A-point	A-point: point of maximum concavity in the midline of the alveolar process of the maxilla
UI(R)	Upper central incisor right: most mesial point of the tip of the crown
UI(L)	Upper central incisor left: most mesial point of the tip of the crown
LI(R)	Lower central incisor right: most mesial point of the tip of the crown
LI(L)	Lower central iincisor left: most mesial point of the tip of the crown
B-point	B-point: point of maximum concavity in the midline of the alveolar process of the mandible
Pg	Pogonion: most anterior midpoint of the chin on the outline of the mandibular symphysis
Me	Menton: most inferior midpoint of the chin on the outline of the mandibular symphysis
PNS	Posterior nasal spine: most posterior midpoint of the posterior nasal spine of the palatine bone
Go(R)	Gonion right: point at the right mandibular angle
Go(L)	Gonion left: point at the left mandibular angle
UM(R)	Upper first molar right: most inferior point of the mesio-buccal cusp of the crown
LM(R)	Lower first molar right: most superior point of the mesio-buccal cusp of the crown
UM(L)	Upper first molar left: most inferior point of the mesio-buccal cusp of the crown
LM(L)	Lower first molar left: most superior point of the mesio-buccal cusp of the crown
Po(R)	Most superior point of the right external acoustic meatus
porion	
Po(L)	Most superior point of the left external acoustic meatus
porion	

to the observers and tracing of each patient was conducted in different sessions with at least 1 day separation to minimize the learning effect. The maximum duration of any individual session was 2 hours. All images were displayed on a 21 inch flat panel screen resolution 1600 × 1200. The lightening conditions were standardized dim yellow lights in a radiology interpretation room.

Statistical analysis

The observations consisted of two measurements of location of each cephalometric point for each combination of patient, observer and tracing method (3D and 3D + MPR). The X, Y, and Z co-ordinates of the two repeated measurements were averaged giving the fiducial location for each landmark.

Figure 2 Example of identifying cephalometric landmarks on three-dimensional surface model in the anterior view (A) and clipped midsagittal (B).

The data were analysed using a mixed model design with fixed factors observer and tracing method and one repeated measurement factor. Fisher's *F*-test was used to test for statistical significant differences between the precision measures (i.e. between 3D and 3D + MPR). Cronbach's α was used to assess inter-observer reliability. All computations necessary for the statistical analyses were done using version 17.0 of the SPSS package (SPSS Inc, Chicago, Illinois, USA). The significance level was set to 0.05.

Results

The precision results for both 3D and 3D + MPR tracings per point are summarized in **Table 2**. There was an overall statistically significant difference in the tracing precision between 3D and 3D + MPR ($P = 0.0001$). 3D + MPR improved the tracing precision in 15 of 22 landmarks; however, it was only statistically significantly more precise in tracing 6 of 22 landmarks (Table 2). Conversely, adding MPR alongside, 3D has measurably reduced the tracing precision of the gonion left and to a lesser extent the upper right and left central incisor points. The total tracing precision irrespective of method ranged between 0.29 ± 0.17 for the upper incisor right and 2.82 (7.53) for the porion right landmark. Inter-observer reliability results as measured by Cronbach's α are summarized in Table 2 and intra-observer reliability results can be found in Table 3. Average time required to trace one patient was 6:03 ± 2:48 and 10:41 ± 4:01 minutes for 3D and 3D + MPR, respectively ($P = 0.0001$).

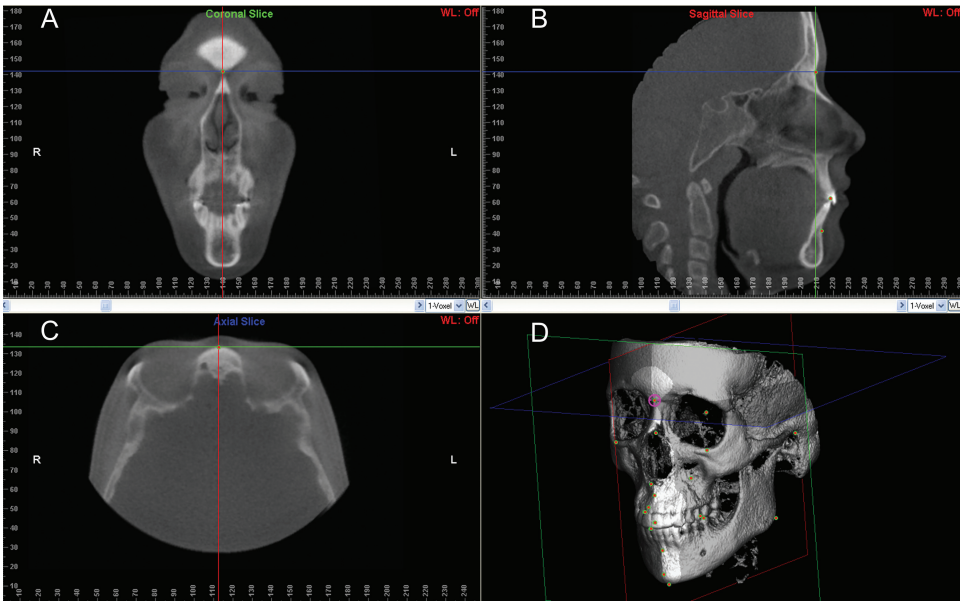

Figure 3 Example of identifying cephalometric landmarks using three-dimensional surface model plus multi-planar reformations using coronal (A), sagittal (B), axial (C) slices, and the three-dimensional model (D).

Table 2 Precision defined as absolute differences in millimetre from mean value and standard deviations of both tracing methods three-dimensional (3D) and [3D + multi-planar reformations (MPR)] per point averaged over all observers.

Structure	3D	3D + MPR	Total precision	*P*	Inter-observer reliability
Orbitale right	1.11 (1.44)	0.89 (0.70)	1.00 (1.14)	0.11	0.06
Orbitale left	1.13 (1.39)	0.86 (0.59)	1.00 (1.07)	**0.04**	0.37
Sella turcica	1.50 (3.70)	0.77 (0.71)	1.13 (2.69)	**0.04**	0.15
Nasion	0.80 (0.86)	0.49 (0.43)	0.64 (0.70)	**0.001**	0.66
Anterior nasal spine	1.20 (3.10)	0.66 (0.53)	0.93 (2.21)	0.06	0.55
Posterior nasal spine	1.16 (1.86)	0.76 (1.11)	0.96 (1.54)	**0.04**	0.58
A-point	0.78 (1.04)	0.64 (0.42)	0.71 (0.80)	0.19	0.28
Upper incisor right	0.27 (0.13)	0.31 (0.20)	0.29 (0.17)	0.07	0.58
Upper incisor left	0.29 (0.20)	0.31 (0.19)	0.30 (0.20)	0.48	0.40
Lower incisor right	0.49 (0.58)	0.48 (0.38)	0.48 (0.50)	0.87	0.69
Lower incisor left	0.74 (1.85)	0.5 (0.45)	0.62 (1.35)	0.19	0.67
B-point	0.77 (0.54)	0.71 (0.44)	0.74 (0.50)	0.3	0.27
Pogonion	0.81 (0.85)	0.72 (0.77)	0.77 (0.81)	0.42	0.57
Menton	1.21 (2.01)	0.78 (0.94)	1.0 (1.58)	**0.03**	0.49
Gonion right	0.87 (0.64)	0.89 (0.60)	0.88 (0.62)	0.77	0.21
Gonion left	0.94 (1.33)	1.21 (3.18)	1.08 (2.44)	0.41	0.09
Upper right molar	0.97 (3.40)	0.99 (3.39)	0.98 (3.39)	0.95	−0.33
Upper left molar	0.65 (1.03)	0.58 (0.76)	0.62 (0.90)	0.58	0.25
Lower right molar	1.51 (3.58)	1.09 (3.16)	1.30 (3.38)	0.34	−0.05
Lower left molar	1.66 (4.21)	0.72 (0.83)	1.19 (3.07)	**0.02**	0.05
Porion left	1.93 (2.76)	1.50 (1.65)	1.72 (2.28)	0.14	0.03
Porion right	3.56 (9.06)	2.09 (5.52)	2.82 (7.53)	0.13	0.06

Total precision per point averaged over both tracing methods and observers. Statistically significant differences in *P* are written in **bold**. Inter-observer reliability as measured by Cronbach's α.

Table 3 Precision defined in millimetre as absolute differences and standard deviation from mean value of both tracing methods three-dimensional (3D) and [3D + multi-planar reformations (MPR)] per observer averaged over all points.

Observer	3D	3D + MPR	Total
1	0.59 (0.63)	0.53 (0.49)	0.56 (0.56)
2	1.36 (4.30)	1.05 (3.79)	1.2 (4.05)
3	1.26 (3.35)	0.95 (2.12)	1.1 (2.8)
4	1.36 (2.33)	0.83 (0.76)	1.09 (1.75)
5	0.89 (1.21)	0.77 (0.90)	0.82 (1.06)
6	2.37 (5.85)	1.47 (3.11)	1.92 (4.69)
7	0.74 (0.62)	0.61 (0.48)	0.67 (0.56)
8	0.50 (0.49)	0.46 (0.37)	0.48 (0.43)
9	0.83 (1.28)	0.66 (0.70)	0.75 (1.03)
10	1.42 (3.98)	0.92 (2.29)	1.17 (3.25)
11	0.86 (1.00)	0.71 (0.73)	0.78 (0.88)

Discussion

The study aim was to assess the precision of identifying cephalometric landmarks on CBCT *in vivo* on both 3D surface models and MPR images. The study results indicate that adding MPR images does indeed seem to increase the precision of identifying cephalometric landmarks and intra- and inter-observer agreement (Tables 2 and 3). However, the tracing time required nearly doubled when using 3D + MPR albeit that it remained under 15 minutes per patient. Tracing midsagittal structures by using MPR sagittal slices closely resembles tracing conventional cephalograms and that may explain the result that four of six statistically improved tracings were midsagittal plane points (Table 2). There is also the possibility that those structures were not clearly visible on the 3D models alone. Thin pointed structures such as ANS and PNS can be extremely threshold sensitive. Moreover, it is well known that in CBCT bone density and therefore its visibility on an isosurface is dependent on its location in the skull due to beam hardening artefacts (Loubele *et al.*, 2007; Liang *et al.*, 2009; Hassan *et al.*, 2010).

It has been previously stated that 3D landmark identification is more precise with MPR yet more time consuming since it requires identifying landmarks on axial, coronal, and sagittal views and double checking the visualization in the three planes of space (Ludlow *et al.*, 2009). A recent study stated that 3D landmark identification with CBCT reconstructions can offer a consistent and reproducible measurement if a protocol for operator training is followed. In that study, the intra-class correlation coefficient (ICC) of three repeated measures of 30 cephalometric points made by three observers were reported (De Oliviera *et al.*, 2009). Their ICC results, although with fewer observers, suggest the presence of systematic variability among the measurements as well. In this study, the residents who performed the tracings were trained in using the software in order to improve the reliability of the measurements. Yet, there was notable variability in the tracing precision of the different observers (Table 3).

The relatively variable standard deviations and the presence of outliers for different points coupled with variable reliability results of the different observers suggest that there is a certain level of noise on the measurements. While imprecise observer measurements can always be attributed as a contributing factor. It could equally be argued that the definitions of those 3D landmarks, which are largely adapted from their 2D definitions, are inadequate for precise tracing on a 3D skull representation. The margin for error in 3D is higher since points are defined in the X, Y, and Z axis instead of the traditional X and Y in 2D. There is currently very little evidence on the clinical significance of measurements imprecision in 3D cephalometry. In traditional, clinical 2D cephalometrics, a landmark error below 1 mm is considered a precise measurement (Richardson, 1981). Whether this measure is applicable in 3D cephalometrics might be questionable since in 3D, a third axis is introduced, which may add additional error to the overall error. However, it has been previously argued that lack of precision in landmark identification may not preclude a proper diagnosis (Lou *et al.*, 2007). This claim is yet to be verified.

Previous *in vitro* and *in vivo* studies did not address the distinction between MPR and 3D models for precision of tracing except in one previous *in vitro* study (Hassan *et al.*, 2009). Also, the time required to conduct 3D cephalometric tracing was not previously quantified. This study was limited that only one IIT CBCT system was investigated with very specific scan and reconstruction settings. Other flat panel detector systems can vary with respect to image quality parameters and settings. Also, the study was limited by the ability of the observers to identify the cephalometric landmarks and the accuracy of the measurements of Dolphin software. The measurements of each patient between 3D and 3D + MPR were also dependent since the 3D co-ordinates were used as starting point and the MPR was added for adjustment. The observed improved precision of tracing in 3D + MPR could have also been affected by the second view of the observers to the data (historical bias). It would have been more objective to allow the observers to trace in 3D and 3D + MPR in different sessions. However, it was deemed that the tracing scenario adopted in this study best mimics the clinical situation in practice.

Finally, the largest imprecision in this study was that of the porion point, which was also observed in a previous study (Ludlow *et al*., 2009). In that study, variability was broken out into anterio-posterior (A/P), medio-lateral (M/L), and caudal-cranial (C/C) directions. Variability of the porion was greatest in the M/L direction (7.1 mm) and secondarily the C/C direction (3.5 mm). Because of the curvature of the external auditory canal (EAC) as it transitions into the temporal surface, the definition of this landmark as the 'most superior point of the external acoustic meatus' is problematic in 3D and MPR views. Also, the lower border of the EAC often terminates at a more medial position than does the upper boarder of the EAC. If an observer locates porion at the most lateral position of a completely circumscribed (bony housing) EAC, this may be more medial and more inferior to the use of only the superior margin of the EAC.

Conclusions

The precision of identifying cephalometric landmarks with CBCT ranges between 0.29 ± 0.17 and 2.82 ± 7.53 and is variable with respect to the landmark location. Addition of MPR does have a positive influence on precision, but it takes on average twice as much time. Whether this more time-consuming tracing method is worthwhile depends on the level of accuracy required, which still needs to be investigated further.

Funding

The authors declare they received no grant for undertaking the study and that no funding from any external institute or commercial interest was provided. The purchase of Dolphin software was financially supported by the section of Orthodontics, Department General and Specialized Dentistry at ACTA.

References

Arai Y, Tammisalo E, Iwai K, Hashimoto K, Shinoda K 1999 Development of a compact computed tomographic apparatus for dental use. Dentomaxillofacial Radiology 28: 245–248

Berco M, Rigali P H, Miner R M, DeLuca S, Anderson N K, Will L A 2009 Accuracy and reliability of linear cephalometric measurements from cone-beam computed tomography scans of a dry human skull. American Journal of Orthodontics and Dentofacial Orthopedics 136: 17.e1–17.e9

Chien P C, Parks E T, Eraso F, Hartsfield J K, Roberts W E, Ofner S 2009 Comparison of reliability in, anatomical landmark identification using two-dimensional, digital cephalometrics and three-dimensional cone beam computed tomography in vivo. Dentomaxillofacial Radiology 38: 262–273

De Oliveira A E, Cevidanes L H, Phillips C, Motta A, Burke B, Tyndall D 2009 Observer reliability of three-dimensional cephalometric landmark identification on cone-beam computerized tomography. Oral Surgery, Oral Medicine, Oral Pathology, Oral Radiology, and Endodontics 107: 256–265

Halazonetis D J 2005 From 2-dimensional cephalograms to 3-dimensional computed tomography scans. American Journal of Orthodontics and Dentofacial Orthopedics 127: 627–637

Hassan B, Couto Souza P, Jacobs R, de Azambuja Berti S, van der Stelt P 2010 Influence of scanning and reconstruction parameters on quality of three-dimensional surface models of the dental arches from cone beam computed tomography. Clinical Oral Investigations 14: 303–310

Hassan B, van der Stelt P, Sanderink G 2009 Accuracy of three-dimensional measurements obtained from cone beam computed tomography surface-rendered images for cephalometric analysis: influence of patient scanning position. European Journal of Orthodontics 31: 129–134

Hilgers M L, Scarfe W C, Scheetz J P, Farman A G 2005 Accuracy of linear temporomandibular joint measurements with cone beam computed tomography and digital cephalometric radiography. American Journal of Orthodontics and Dentofacial Orthopedics 128: 803–811

Kau C H, Richmond S, Palomo J M, Hans M G 2005 Three-dimensional cone beam computerized tomography in orthodontics. Journal of Orthodontics 32: 282–293

Kragskov J, Bosch C, Gyldensted C, Sindet-Pedersen S 1997 Comparison of the reliability of craniofacial anatomic landmarks based on cephalometric radiographs and three-dimensional CT scans. Cleft Palate-Craniofacial Journal 34: 111–116

Kumar V, Ludlow J, Cevidanes L H S, Mol A 2008 In Vivo comparison of conventional and cone beam CT synthesized cephalograms. Angle Orthodontist 78: 873–879

Kumar V, Ludlow J B, Mol A, Cevidanes L 2007 Comparison of conventional and cone beam CT synthesized cephalograms. Dentomaxillofacial Radiology 36: 263–269

Lagravère M O, Carey J, Toogood R W, Major P W 2008 Three-dimensional accuracy of measurements made with software on cone-beam computed tomography images. American Journal of Orthodontics and Dentofacial Orthopedics 134: 112–116

Liang X *et al.* 2009 A comparative evaluation of Cone Beam Computed Tomography (CBCT) and Multi-Slice CT (MSCT). Part II: on 3D model accuracy. European Journal of Radiology 75: 270–274

Lou L, Lagravere M O, Compton S, Major P W, Flores-Mir C 2007 Accuracy of measurements and reliability of landmark identification with computed tomography (CT) techniques in the maxillofacial area: a systematic review. Oral Surgery, Oral Medicine, Oral Pathology, Oral Radiology, and Endodontics 104: 402–411

Loubele M, Guerrero M E, Jacobs R, Suetens P, van Steenberghe D 2007 A comparison of jaw dimensional and quality assessments of bone characteristics with cone-beam CT, spiral tomography, and multi-slice spiral CT. International Journal of Oral Maxillofacial Implants 22: 446–454

Loubele M *et al.* 2008a Image quality vs radiation dose of four cone beam computed tomography scanners. Dentomaxillofacial Radiology 37: 309–319

Loubele M, Maes F, Jacobs R, van Steenberge D, White S C, Suetens P 2008b Comparative study of image quality for MSCT and CBCT scanners for dentomaxillofacial radiology applications. Radiation Protection Dosimetry 129: 222–226

Ludlow J B, Gubler M, Cevidanes L H, Mol A 2009 Precision of cephalometric landmark identification: cone-beam computed tomography vs conventional cephalometric views. American Journal of Orthodontics and Dentofacial Orthopedics 136: 312.e1–312.e10

Ludlow J B, Ivanovic M 2008 Comparative dosimetry of dental CBCT devices and 64-slice CT for oral and maxillofacial radiology. Oral Surgery, Oral Medicine, Oral Pathology, Oral Radiology, and Endodontics 106: 106–114

Lundström A, Lundström F, Lebret L M, Moorrees C F 1995 Natural head position and natural head orientation: basic considerations in cephalometric analysis and research. European Journal of Orthodontics 17: 111–120

Maeda M *et al.* 2006 3D-CT evaluation of facial asymmetry in patients with maxillofacial deformities. Oral Surgery, Oral Medicine, Oral Pathology, Oral Radiology, and Endodontics 102: 382–390

Marmulla R, Wörtche R, Mühling J, Hassfeld S 2005 Geometric accuracy of the NewTom 9000 Cone Beam CT. Dentomaxillofacial Radiology 34: 28–31

Moshiri M, Scarfe W C, Hilgers M L, Scheetz J P, Silveira A M, Farman A G 2007 Accuracy of linear measurements from imaging plate and lateral cephalometric images derived from cone-beam computed tomography. American Journal of Orthodontics and Dentofacial Orthopedics 132: 550–560

Olszewski R, Cosnard G, Macq B, Mahy P, Reychler H 2006 3D CT-based cephalometric analysis: 3D cephalometric theoretical concept and software. Neuroradiology 48: 853–862

Palomo J M, Rao P S, Hans M G 2008 Influence of CBCT exposure conditions on radiation dose. Oral Surgery, Oral Medicine, Oral Pathology, Oral Radiology, and Endodontics 105: 773–782

Periago D R, Scarfe W C, Moshiri M, Scheetz J P, Silveira A M, Farman A G 2008 Linear accuracy and reliability of cone beam CT derived 3-dimensional images constructed using an orthodontic volumetric rendering program. Angle Orthodontist 78: 387–395

Pinsky H M, Dyda S, Pinsky R W, Misch K A, Sarment D P 2006 Accuracy of three-dimensional measurements using cone-beam CT. Dentomaxillofacial Radiology 35: 410–416

Richardson A 1981 A comparison of traditional and computerized methods of cephalometric analysis. European Journal of Orthodontics 1: 15–20

Roberts J A, Drage N A, Davies J, Thomas D W 2009 Effective dose from cone beam CT examinations in dentistry. British Journal of Radiology 82: 35–40

Silva M A G, Wolf U, Heinicke F, Bumann A, Visser H, Hirsch E 2008 Cone beam computed tomography for routine orthodontic treatment planning: a radiation dose evaluation. American Journal of Orthodontics and Dentofacial Orthopedics 133: 640.e1–640.e5

Suomalainen A, Kiljunen T, Käser Y, Peltola J, Kortesniemi M 2009 Dosimetry and image quality of four dental cone beam computed tomography scanners compared with multislice computed tomography scanners. Dentomaxillofacial Radiology 38: 367–378

Swennen G R J, Schutyser F 2006 Three-dimensional cephalometry: spiral multi-slice vs cone-beam computed tomography. American Journal of Orthodontics and Dentofacial Orthopedics 130: 410–416

Swennen G R J, Schutyser F, Barth E, De Groeve P, De Mey A 2006a A new method of 3-D cephalometry Part I: the anatomic cartesian 3-D reference system. Journal Craniofacial Surgery 17: 314–325

Swennen G R J, Schutyser F, Hausamen J 2006b Three-dimensional cephalometry. A color atlas and manual. Springer-Verlag, Berlin